

AIR-GAP REDUCTION AND ANTENNA POSITIONING OF AN X-BAND BOW TIE SLOT ANTENNA ON 2U CUBESATS

Boutaina Benhmimou¹, Fouad Omari², Nancy Gupta³, Khalid El Khadiri⁴, Rachid Ahl Laamara⁵, Mohamed El Bakkali^{6*}

LPHE-MS, Faculty of Sciences, University Mohammed V in Rabat (UM5), Rabat, Morocco^{1,2,5,6}

ECE Department, Lyallpur Khalsa College Technical Campus, Jalandhar, Punjab, India³

Department of Physics, Faculty of Sciences El Jadida, University Chouaib Doukkali of El Jadida, Morocco^{4,6}

mohamed.elbakkali1617@gmail.com

Received: 23 September 2024, Revised: 16 November 2024, Accepted: 19 November 2024

*Corresponding Author

ABSTRACT

In this research work, a small size and wide-band Bow Tie slot antenna (BTSA) is proposed and optimized for use on an unlimited lifetime small-sized CubeSats at X-band. Interestingly, this paper introduces a graceful mechanism of integrating Bow Tie slot antennas on the bodies of small CubeSat configurations, which minimizes the antenna throwing from the satellite body and the whole CubeSat volume. The proposed approaches propose and analyze in detail how a small metallic part of a 2U CubeSat body improves the antenna performances around an operating frequency of 8.4 GHz. It maximizes the antenna gain simultaneously with the beamwidth angles at 8.4 GHz by suppressing the resulting back-lobes, which are re-directed outside the CubeSat box. These impacts are achieved by shifting a very small air-gap distance of only 1 mm between the back face of the BTSA dielectric and the CubeSat top face. The developed BTSA is lightweight and exhibits a unidirectional radiation pattern with a wide beamwidth angle of about 160° and a high gain of about 11.0 dBi at 8.4 GHz. The overall results with occupied size and volume are satisfactory for unlimited lifetime CubeSat missions at X-band such as UM5-Ribat and UM5-EOSAT of University Mohammed V in Rabat.

Keywords: Air-Gap Distance, Bow Tie Slot Antennas, High Stiffness Cubesat Antenna, Cubesat Lifetime.

1. Introduction

Until the early twentieth century, developing space technology and satellite engineering projects in developing and emerging countries did not have a significant impact on long-term economic well-being. In light of this, the emergence of cubic satellites and their accelerated development as less expensive spacecraft in construction and manufacturing than conventional satellites alerted the scientific research community to the importance of investing in these satellites for everyday use (Campioli et al., 2024). CubeSats have the potential to make significant economic and cultural contributions, prompting people to regard them as part of their future collective awareness (Abels, 2024). CubeSats are now launched into orbit through cooperative commercial launches at a lower cost than conventional satellites (Jardak & Adam, 2023). Many research teams were driven to develop cubic satellite technology or build their own launch services (El Bakkali, 2020). Experienced engineers have been able to build a common standard for cubic satellites that makes their preparation less expensive and takes only a few weeks to incorporate into training for further growth and education (Voštinár et al., 2023). The low cost of satellite projects and engineering properties has piqued the interest of numerous educational institutions worldwide, including the University of Mohammed V in Rabat (UM5-Ribat and UM5-EOSAT, 2024). Around the world, there are several yearly events that provide students the chance to learn about the creation of these new satellites and exchange stories (Chin et al., 2017).

The conventional design for cubic satellites is one unit (1U), which is a cube that is 10 cm long on each side and weighs around 1.3 kg (Francisco et al., 2023) (Cratere et al., 2024). PSLV C18 was one of several launch vehicles that carried secondary payloads into orbit (El Bakkali et al., 2020). Moreover, advances in technology have made it possible to build ultra-small satellites for remote measurement and various space experiments using a variety of integrated and reliable autonomous equipment. Hence, the communications system of a CubeSat is its

most crucial part; it transmits measurements to ground stations and accepts remote orders from customers (Huang et al., 2024). It is important to stress that mission requirements dictate the electrical and physical features of the cubic satellite telecommunications system, and vice versa. Furthermore, just a few minutes per day are spent in communication between the ground stations and the cubic satellite. However, because the satellite moves so quickly, it becomes more challenging to communicate with ground stations. Furthermore, the majority of cubic satellite projects can only supply one or two earth stations with three meters of antennas; thus, the download speed may hinder these plants' low power. However, because the satellite's angle changes when it moves, the angle of divergence from toxicity could also shift. Therefore, cubic satellite antennas need to be high gain, occupy geometrically suitable dimensions, and function well on a frequency that enables high-data-rate, long-range transmission.

New antenna systems that can fulfill the requirements of high data rate and accuracy while also increasing the system's physical dimensions are being actively developed by the scientific community in order to be used even on deep space missions. Bipolar antennas must be installed once cubic satellites are sent into orbit in order for several of them to communicate with base stations. Thus, the entire task fails if the deployment mechanism malfunctions. Therefore, level antennas are a superior choice for usage on cubic spacecraft in terms of engineering and mechanics (El Bakkali et al., 2021). It may be readily integrated with other cubic satellite tools and is inexpensive, lightweight, and low in height (Liu & Feng, 2023; Liu et al., 2024; Chu et al., 2023; Zhang et al., 2023). Numerous strategies have been put out to increase level antennas' overall gain and bandwidth in order to satisfy deep space mission requirements. As the antenna's mass and weight rise, the majority of them rely on adding new components. On the other hand, this message aims to design and construct a tiny aperture antenna powered by a 50Ω strip line that is integrated into the body of a second unit cubic satellite, without the need for additional components, an increase in antenna power, or any secondary deployment. By cutting the air gap between the made antenna's body and the rear of the cubic satellite by just around 1 mm, with an area that does not exceed 8% of the antenna's back, you may basically increase the group's overall stiffness. However, by using the satellite's own back as a reflector and only properly positioning the antenna, the authors aim to increase the antenna peak gain at 8.4 GHz (El Bakkali, 2020). More particularly, the authors want to incorporate the Bow Tie aperture antenna on the rear of a cubic spacecraft for the first time, attaining the following primary objectives.

1. Improve and minimize the size of the Bow Tie aperture antenna to occupy less than 8% of the grand interface of a second unit cubic satellite, with the remainder of the space devoted to other components such as solar power kits, radars, surveillance, and sensor systems.
2. Figure 1 shows how the antenna's performance around the considered resonant frequency is affected by its placement on the broader surface of the aluminum CubeSat box. This implies that the aluminum box will serve as a reflector to enhance antenna characteristics and lessen overlaps with other subsystems. To achieve these qualities, the QNM algorithm is performed to the complete set configuration in order to obtain these properties. The suggested Bow Tie aperture antenna is initially put in the center of the satellite's top face, and displacement is measured along the x, y, and z axes. The QNM algorithm starts at the left edge location and analyzes the full satellite performance at 8.4 GHz. If the requirements are fulfilled, the improvement process is completed, and the final design is appropriate for the CubeSat mission being created. Otherwise, the results are unsatisfactory and then move to the other spots according to the following trinity (x; y, z) for 1000 repeats.
3. Reduce the air gap distance between the CubeSat's upper face and the rear side of the proposed Bow Tie slot antenna, taking into mind the gain and HPBW targets, as well as potential overlaps with other devices. This attribute is required for a high-rigidity satellite to operate in outer space, where it rotates at extreme speeds. This is the most crucial aspect of Bow Tie aperture antennas, which were initially proposed as a viable choice for high data rate CubeSat communications. The authors also hope to show that the peak gain of the group as a whole is inversely proportional to the air distance between them, a feature that is being considered for the first time in the scientific research community, thanks to the nature of the

Bow Tie slot antennas used for the first time on a CubeSat.

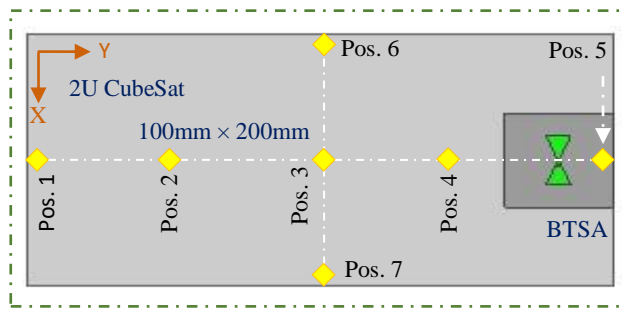


Fig. 1. Antenna Positioning on a 2U CubeSat wider

The above features are being used for the first time on 2U CubeSat designs at X-band with Bow Tie slot antennas. They demonstrate the feasibility of utilizing a very short air gap distance and a small area on the 2U CubeSat top face to achieve outstanding performances at an operational frequency of 8.4 GHz. This paper is organized as follows: Section 2 details geometrical description of proposed Bow Tie Slot antenna design, its optimized dimensions and integration with a 2U CubeSat. This section demonstrates and discusses how the geometrical features for a 2U CubeSat mission are satisfied. Section 3 discusses and analyses the achieved results of proposed approaches in a very detailed parametric analysis. Section 4 studies effectiveness and advantages of proposed Bow Tie Slot antenna for all CubeSat Configurations including the 2U at X-band. This Section introduces also a detailed comparison between our proposed BTSA design and some works on CubeSat antennas that use metasurface and other approaches on X-band patch antennas. Finally, section 5 concludes our contributions presented in this research work with the proposal of some perspectives based on the developed study.

2. Antenna Configuration and Evolution of Proposed Antenna Positioning

An X band Bow Tie slot antenna is developed and optimized using ANSYS HFSS for operation at 8.4 GHz (Patidar et al., 2024) (Giannetti, 2023) while taking into consideration the geometrical restrictions of a 2U CubeSat configuration. This tiny antenna design is printed on the upper surface of the inexpensive Teflon dielectric ($\epsilon_r = 2.1$, $\tan\delta = 0.001$, and $h = 1.2$ mm), which is regarded as a substrate material due to its broad market availability and excellent reliability qualities for higher frequency aerospace applications (Kogut et al., 2022). According to Fig. 2, the suggested Bow Tie antenna arrangement takes up just 6.84% of the top face of a 2U CubeSat construction (10×20 cm²). Additionally, Fig. 3 demonstrates that the Bow Tie slot antenna design that was built has the physical dimensions specified in Table 1. It is fed by a 50- Ω strip line that measures 0.47×0.47 mm² and is positioned at a modest distance of $g = 0.235$ mm from the antenna geometrical center along the X-axis.

Table 1 - Geometrical parameters and antenna positioning of proposed BTSA.

W	L	L1	W1	L2	W2	h
37mm	37mm	10.46mm	8.42mm	10.46mm	8.42mm	1.2mm
Pos.6	Pos.1	Pos.2	Pos.3	Pos.4	Pos.5	Pos.7
(X ; Y ; Z) = (-31.5; 0.5; 30)	(X ; Y ; Z) = (0; 81.5; 1)	(X ; Y ; Z) = (0; 41.5; 1)	(X ; Y ; Z) = (0; 0.5; 1)	(X ; Y ; Z) = (0; -40.5; 1)	(X ; Y ; Z) = (0; -81.5; 1)	(X ; Y ; Z) = (31.5; 0.5; 30)

By using the BTSA technique, designers hope to obtain a very rigid range with a small-area, lightweight antenna that is engineering compatible with all satellites. The design for obtaining high gains and large -10dB bandwidths around 8.4 GHz is further explained by the QNM algorithm, which has been accepted in the course of improvement. By moving the BTSA antenna, which is mounted on the satellite's face, in all directions, the radiating characteristics of the whole CubeSat are computed and enhanced. With antenna characteristics appropriate for a CubeSat flight, the QNM algorithm reduces the separated air gap distance to a limit of just 1 mm. The Whole CubeSat was examined at a second air gap of 30 mm in order to conduct a more thorough investigation.

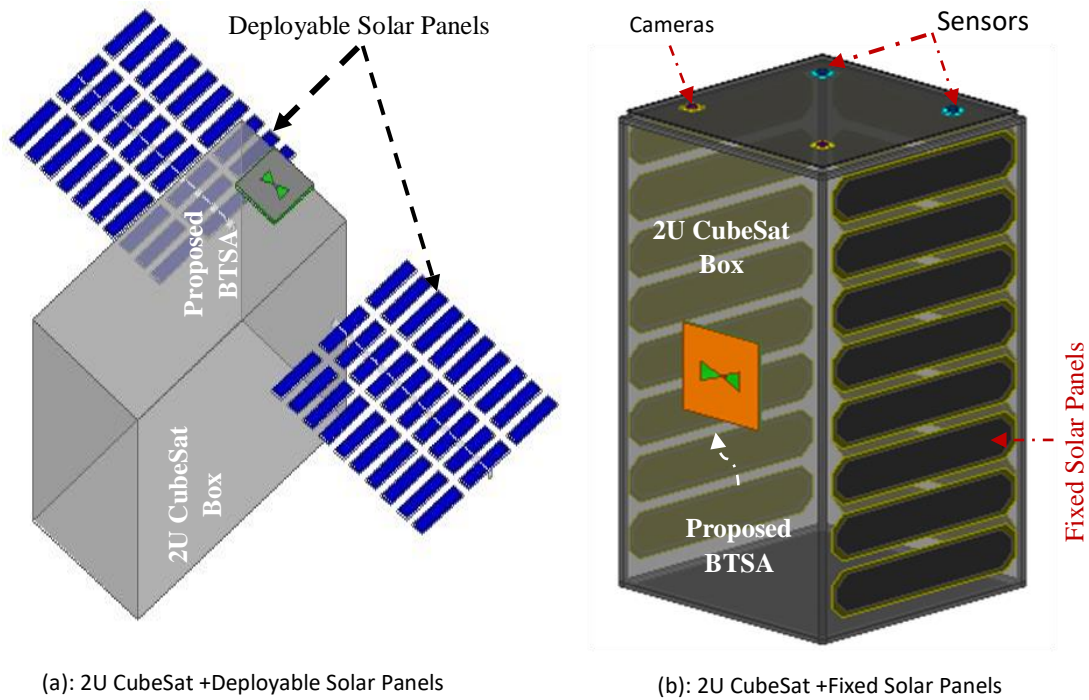


Fig. 2. Layout of developed 2U CubeSat configuration: 2U CubeSat + Proposed BTSA

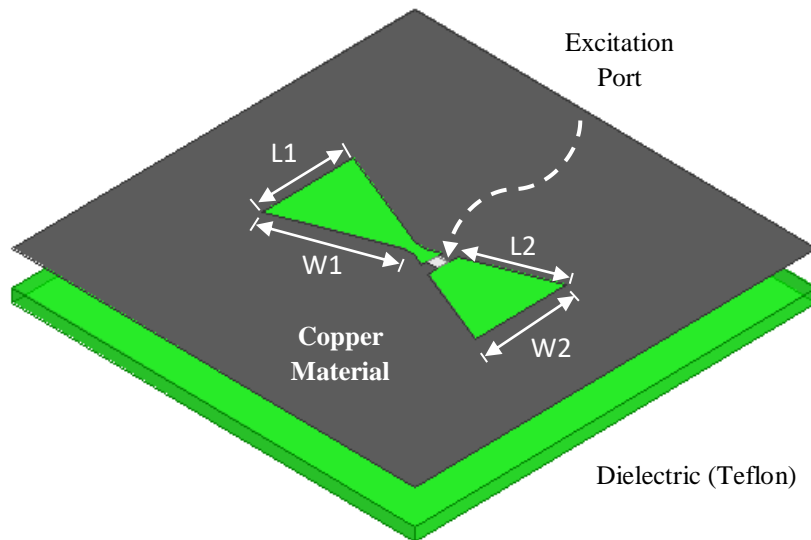


Fig. 3. Dimensions of proposed Bow Tie slot antenna

In comparison to those that may be obtained with a second air gap distance of up to 30 mm, designers were able to achieve the requisite 8.4 GHz precipitation at an air gap distance of no more than 1 mm. The inverse relationship between air gap distance and antenna acquisition at the same resonance frequency serves as evidence for this. This study shows that all geometric and operational barriers, such as size, dimensions, or energy required for operation related to micro-space technology, are practically solvable and even more volatile than anticipated. It also achieves the highest gains at an operating frequency of 8.4 GHz and with a very small air distance of only 1 mm. This inspires the scientific research community to take additional initiatives to advance their own. The Bow Tie slot antenna built on a CubeSat is the first to show this in the scientific research sector.

3. Results Synthesis and Discussion

In this section, radiation characteristics of proposed Bow Tie slot antenna with and without the CubeSat chassis are analyzed in terms of their suitability for unlimited lifetime 2U CubeSat missions. Using the QNM optimization algorithms introduced in this research, the proposed approaches lead to the design of a small size Bow Tie slot antenna having full area $L \times W$ of $37 \times 37 \text{ mm}^2$ and radiation characteristics analyzed around an operating frequency of 8.4 GHz using physical dimensions listed in Table 1. Return loss (RL) and VSWR plots of proposed BTSA antenna structure are depicted in Fig. 4. It is observed that the constructed Bow Tie slot antenna resonates around 8.4 GHz with return loss having peak of about 21 dB at 8.66 GHz and an ultra-wide impedance bandwidth ranging from 7.87 GHz to 9.46 GHz (-10dB BW 1.59 GHz) and VSWR of 1.20 at 8.66 GHz. Therefore, the proposed BTSA configuration can operate well around X-band resonant frequencies close to 8.4 GHz with low excitation power is being reflected back to the excitation source. In addition to that, this small size BTSA presents good distributions of current and E-field while the achieved radiation pattern which is presented in 2D (XY and XZ planes) and 3D is bidirectional at 8.4 GHz. Hence, an important quantity of electromagnetic energy is wasted through the back lobe radiations, see Fig.5 and Fig. 6(a). The back lobe radiations generate interferences with components inside the CubeSat body and hence may increase the mission failure. In addition to that, the achieved radiation pattern takes the horizontal plan as plan of symmetry and hence losses are almost equal to the radiated energy along Z-axis. It proves a very high chance of mission failure due to the interferences between electronic components. Moreover, Fig. 6(b) observes that despite the high losses generated via the back lobe radiation, the developed BTSA structure gives peak gain of 5.92 dBi at 8.4 GHz and then in terms of gain the proposed Bow Tie slot antenna alone is suitable for inter-CubeSat and CubeSat Swarm communications if interferences with components inside the CubeSat box supposedly solved applying the suitable approaches. Moreover, almost 4.0 dBi or above is lost from the peak gain value at 8.4 GHz through the back lobe radiation.

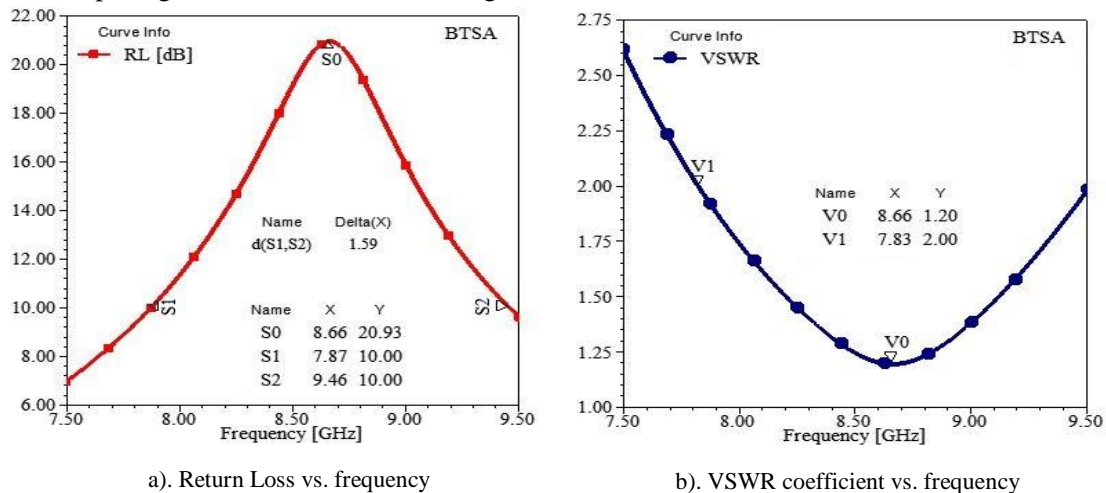


Fig. 4. RL and VSWR coefficients of proposed Bow Tie Slot antenna

The considered BTSA antenna system fills a small area of $37 \times 37 \text{ mm}^2$, is lightweight, low cost and presents very high stiffness configuration that make it a good candidate for all CubeSat standards if the point of interferences with other systems is overcome via a successful approach. The antenna configuration gives suitable return loss (i.e., small $|S_{11}|$), VSWR close to one and very high efficiency at X-band and hence it can be used as very effective solution for CubeSat communications when the rate of mission failure may be minimized as maximum as possible. Interferences and the bidirectional shape of radiation pattern still the only ones that minimize effectiveness of using the proposed Bow Tie slot antenna alone on CubeSats. Its bidirectional radiation pattern shows that an important quantity of electromagnetic energy is radiated in the back direction and so leads to low gains and generates interferences with other subsystems inside the CubeSat box.

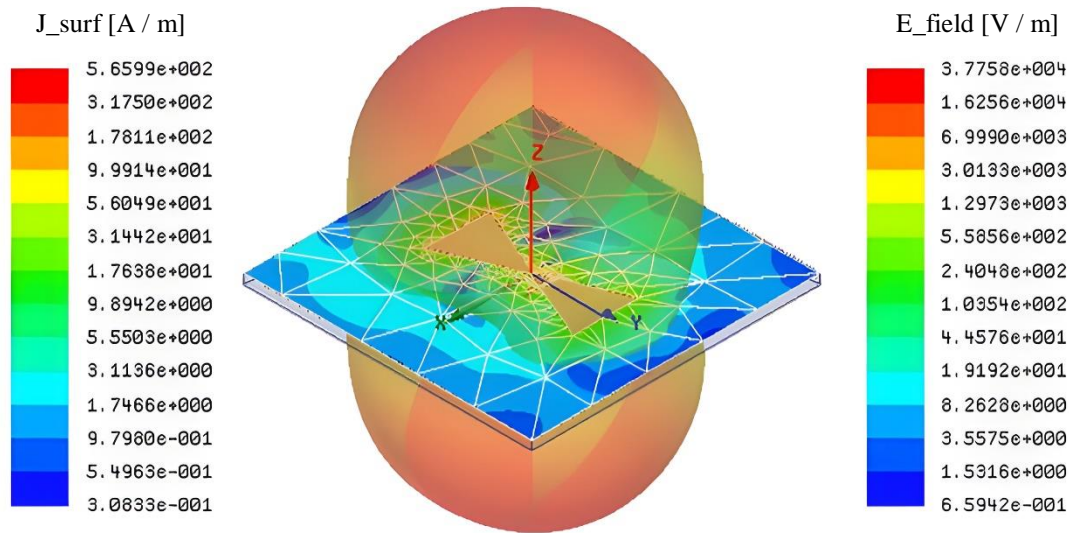
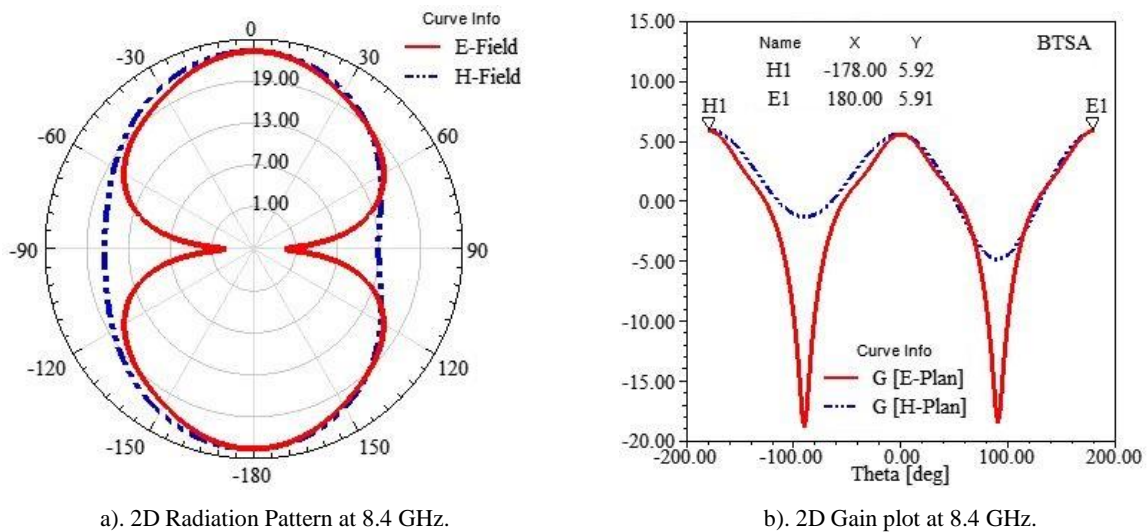


Fig. 5. Reflection and VSWR coefficients of proposed Bow Tie Slot antenna



a). 2D Radiation Pattern at 8.4 GHz. b). 2D Gain plot at 8.4 GHz.

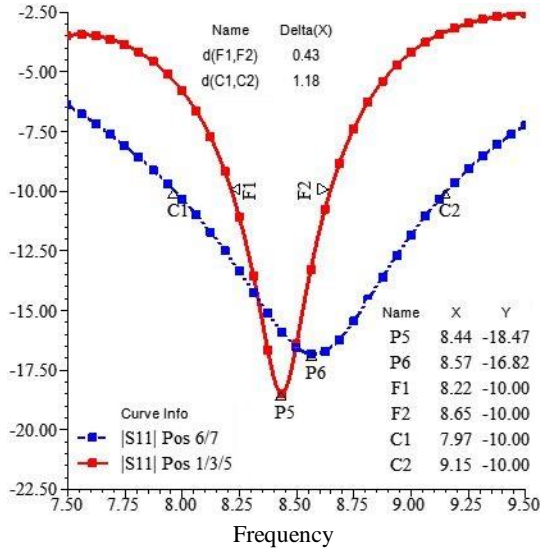
Fig. 6. E-field, H-field, and 2D Gain plots of proposed Bow Tie Slot antenna: 8.4

To deal with these electromagnetic issues, the use of a small part of the CubeSat’s top face as metallic reflector is applied in order to suppress the back lobe radiation and so improves the antenna peak gain at 8.4 GHz up to almost 11.0 dBi. In this regard, antenna positioning on the body of a 2U CubeSat is studied in details taken into consideration the use of a very small air gap distance between the CubeSat top face and the BTSA dielectric back face with operation around the same resonant frequency of 8.4 GHz. Table 2 and Fig. 7(a) show how this antenna approach gives reflection coefficient well below -18.0 dB at 8.44 GHz with wide impedance bandwidths for five fundamental antenna positions along X and Y axes using only an air gap distance of 1mm. Similar performances are assessed at a second air gap distance of 30mm, and it is discovered that the return loss and peak gain vs air gap distance evolve inversely or arbitrarily. In other words, extremely tiny air gap distances can affect the shape of radiation patterns, resulting in improved performances when compared to very large air gap distances. This principle is extremely essential in CubeSat antenna design since it results in reduced volume and high stiffness antenna arrangements. Furthermore, the use of antennas outside the CubeSat body reduces the necessity for excellent impedance matching at the CubeSat’s working frequency. Furthermore, since just a few ground stations communicate with a CubeSat unit, a few hundreds of MHz are adequate for impedance bandwidths and hence the form of the radiation pattern, with HPBW and antenna peak gain being the primary antenna characteristics

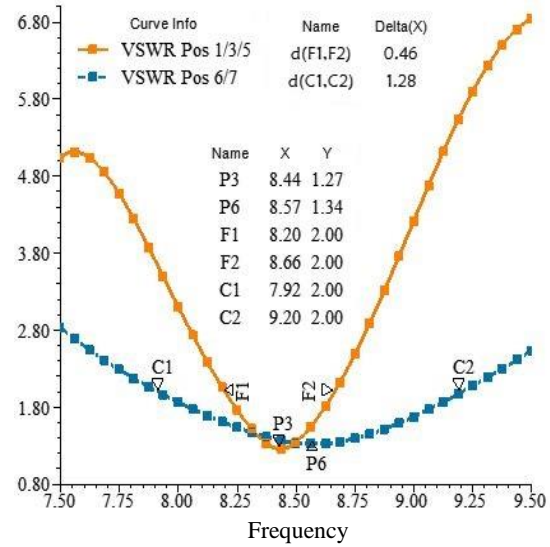
for CubeSat applications. The results of the VSWR coefficient given in Fig. 7(b) and the features described in Figs. 8 and 9 confirm the same recommendations for the same operating frequency of 8.4 GHz.

Table 2 - Reflection coefficient, VSWR and -10dB BW of proposed full system vs. antenna positions.

Ant. positioning	Pos. 7	Pos. 1	Pos. 2	Pos. 3	Pos. 4	Pos. 5
(X; Y; Z)	(31.5;0.5;30)	(0;81.5;1)	(0;41.5;1)	(0;0.5;1)	(0;-40.5;1)	(0;-81.5;1)
F ₀ in GHz	8.54	8.44	8.43	8.43	8.43	8.43
S ₁₁ (dB)	-17.33	-18.46	-18.10	-18.73	-18.27	-18.84
BW (GHz)	7.94- 9.19	8.22- 8.65	8.21-8.64	8.21- 8.65	8.2- 8.64	8.21- 8.65



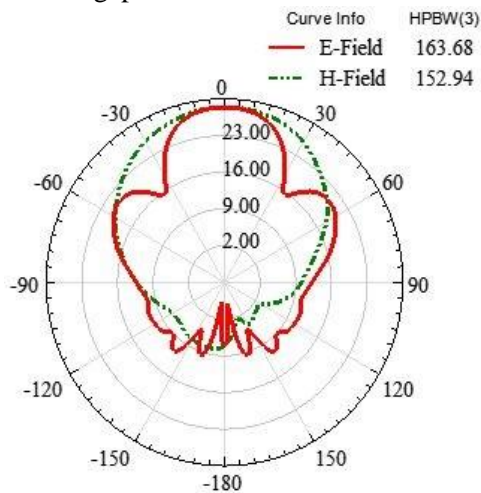
a). Reflection coefficient vs. Frequency



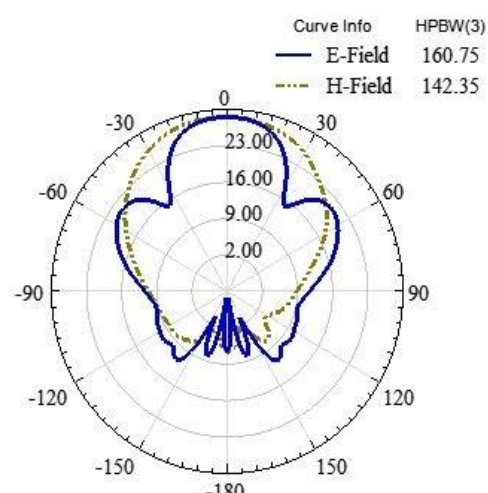
b). VSWR coefficient vs. Frequency

Fig. 7. Reflection and VSWR coefficients of proposed 2U CubeSat configuration.

It is observed that the proposed Bow Tie slot antenna system mounted on the body of a 2U CubeSat radiates unidirectionally at 8.4 GHz for the five antenna positions that are studied at 1mm air gap distance along X, and Y-axis. However, it is proved that the long air gap distance between the antenna dielectric and the CubeSat box (i.e., 30mm) generates high-level back lobes whereas it leads to low stiffness and hence would imply a rate of mission failure. The air gap distance of 1mm achieves the highest antenna stiffness with unidirectional radiation pattern, very wide beamwidth angle for both E and H-planes and high gain of about 11 dBi at 8.4 GHz, see Figs. 10 and 11. Hence, integrating the proposed BTSA design with a 2U CubeSat at an only 1mm air gap distance leads to obtain the desired features for an excellent CubeSat mission.



a). Antenna Position 1: (X; Y; Z) = (0; 81.5; 1)



b). Antenna Position 2: (X; Y; Z) = (0; 41.5; 1)

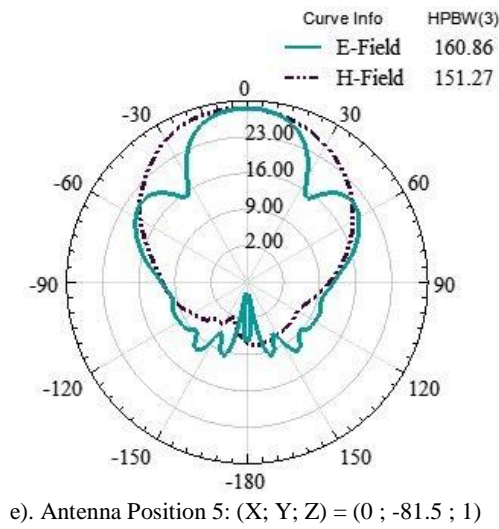
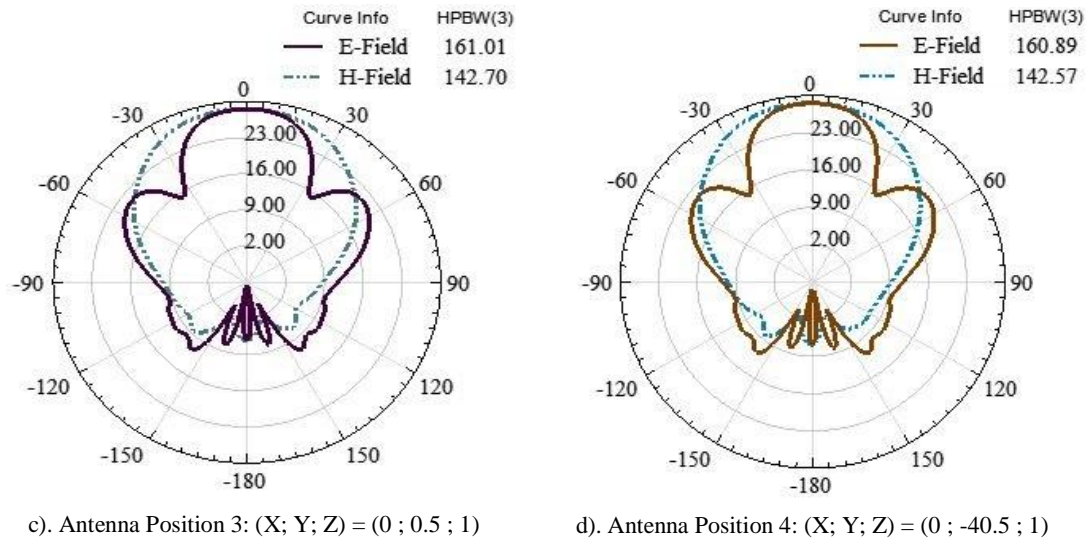


Fig. 8. E- and H- fields of proposed 2U CubeSat at 1mm: 8.4 GHz; [Phi=0°; 90°].

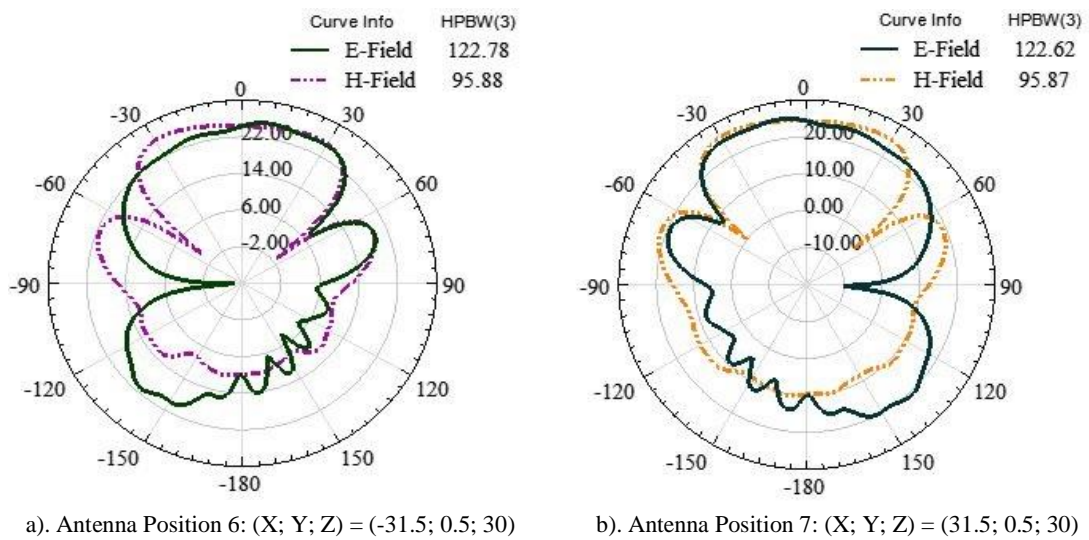


Fig. 9. E- and H- fields of proposed 2U CubeSat at 30mm: 8.4 GHz and [Phi=0°; 90°].

We can say, therefore, that the proposed lightweight and small size BTSA antenna system promotes the ability of building simultaneous transmission links with several earth segments and other CubeSats taken into consideration the area/energy-saving for multiple tasks by not

increasing the physical size and power consumption of proposed BTSA configuration. In addition to that, it is proved that the suppression of back lobe radiation and gain enhancement evolve inversely with the air gap distance. This recommendation is the first time obtained using slot antennas for CubeSats. It is due to the special configuration of Bow Tie slot antennas as compared with other shape of slot antennas. As it is mentioned in Figs. 10 and 11, results of peak gains for all cited antenna positions lead to recommend the same achievements. It is found that the air distance of 1mm gives peak gains of almost 11.0 dBi at 8.4 GHz while using 30 mm achieves peak gains smaller than 8.5 dBi despite the high volume of constructed designs.

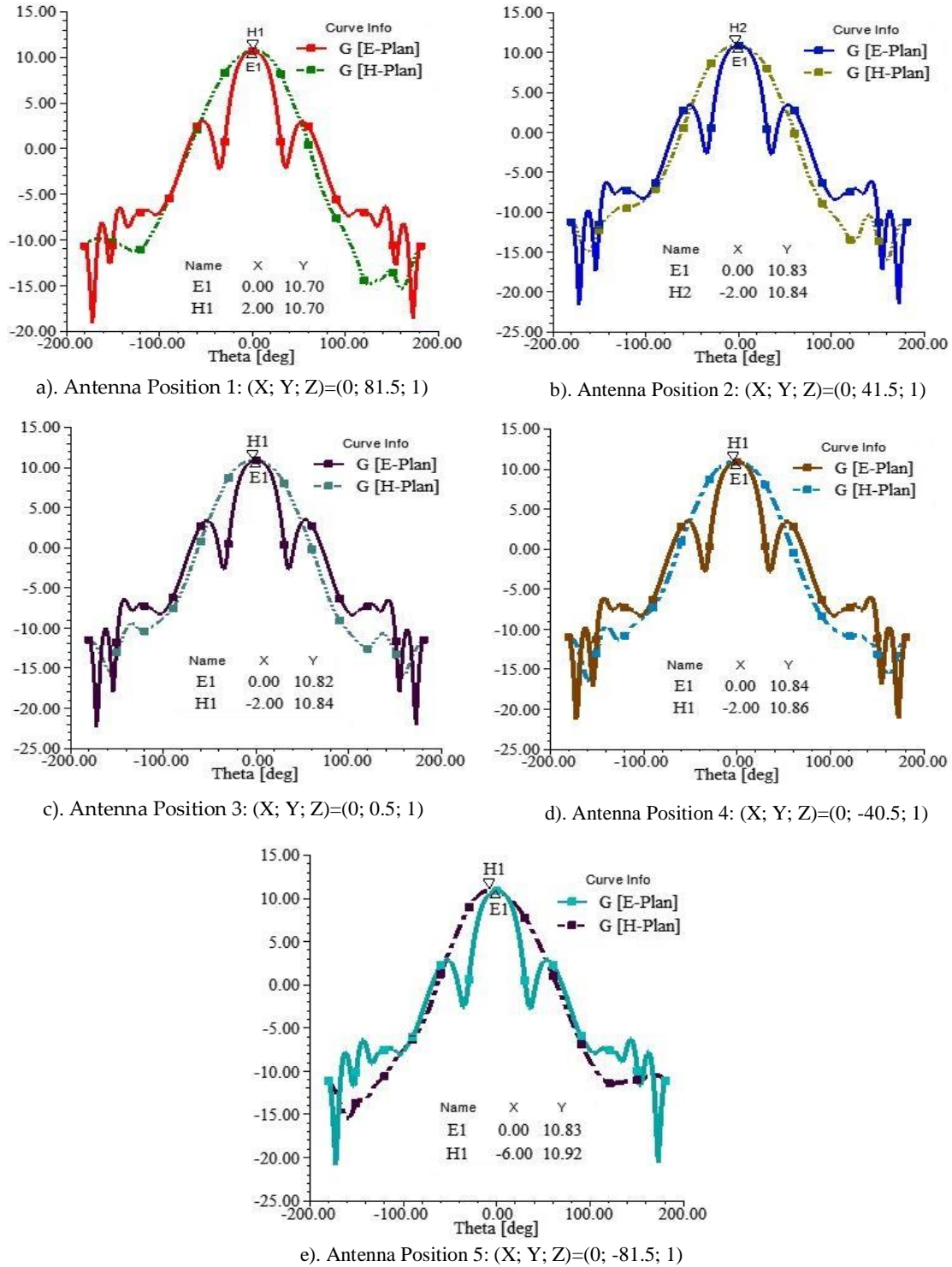


Fig.10. 2D gain of proposed 2U CubeSat mission at an air gap of 1mm: 8.4 GHz.

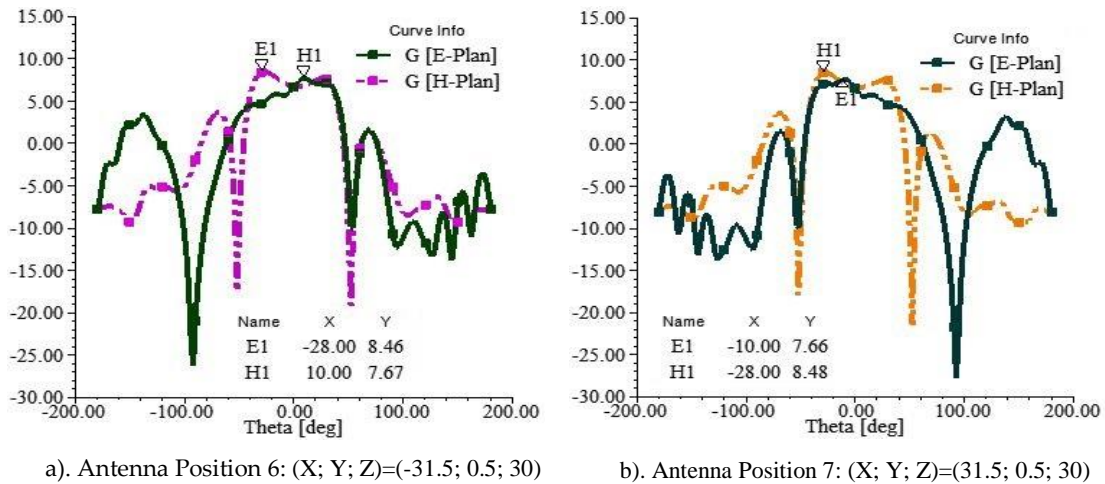


Fig. 11. 2D gain of proposed 2U CubeSat mission at an air gap of 30mm: 8.4 GHz.

Fig.12 observes current distribution of proposed full CubeSat configuration at 8.4 GHz and proves the same conclusions at 1mm air gap distance with minimum interferences between the constructed Bow Tie slot antenna and other instruments inside the CubeSat box. Wherefore, it is obvious to wrap up that the major effects of using a small metallic part below the BTSA rear side to re-focus electromagnetic energy backed inside the CubeSat as back lobes and hence increasing field, as high as possible, outside the CubeSat and perpendicularly with its top face where the proposed antenna is welded. This allows enhancing the antenna gain and eliminating interferences with other electronic components using very small air interstice thickness of 1mm. This means that the maximum energy is radiated into space after integrating the proposed Bow Tie slot antenna with the box of a 2U CubeSat with the ability of high data rate communication with several ground stations on the earth surface.

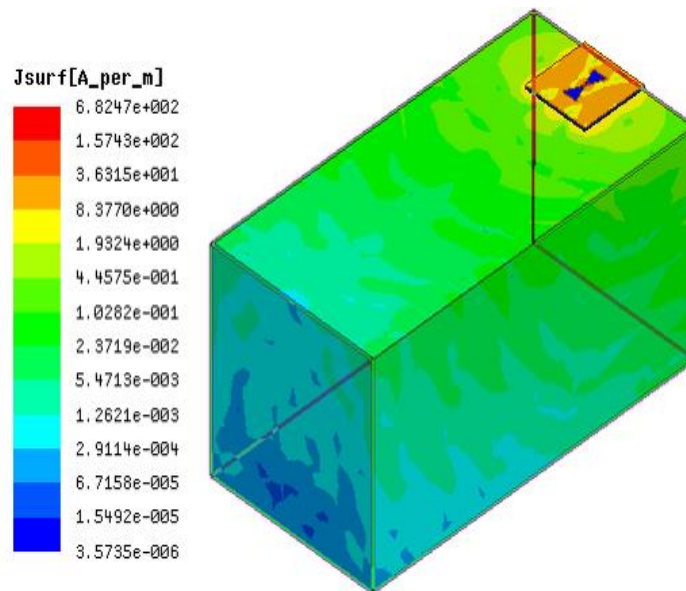


Fig. 12. Current distribution of proposed 2U CubeSat configuration at 8.40 GHz

The developed Bow Tie slot antenna mounted on the box of a 2U CubeSat is low cost, lightweight, wide-band, and achieves good return loss ($|S_{11}|$ close to -20.0 dB) with peak gain of about 11.0 dBi, wide HPBW of almost 160° and very high efficiency (i.e., 99%) around a centered CubeSat frequency of 8.40 GHz.

4. Summary of achieved Results and Brief Comparisons with Literature Works

In this section, the achieved results are summarized in tables 3 and 4 and are studied according to their suitability for 0.5U, 1U, 2U, 3U and 6U CubeSat configurations for a more comprehensive study. The configured BTSA system is lightweight, very small volume, low

cost, high stiffness and occupies small area on the CubeSat body. Therefore, geometrically and mechanically, it is very suitable for all CubeSat configurations. Electrically, this antenna design gives high gain of about 11.0 dBi, wide HPBW (~160°), and wide -10dB BW which are very efficient for unlimited lifetime CubeSat missions at X-band. This means that the developed 2U AeroCube configuration can be used for hundreds of years after the satellite launch due to the absence of atmospheric drag at high altitudes, small sectorial area, low mass, high antenna gain and wide HPBW of proposed 2U CubeSat. In addition to that, the other CubeSat configuration can be targeted as high altitude satellite missions using the constructed Bow Tie slot antenna system since their masses and sectorial areas are close to each other. From another hand, the achieved wide band and wide HPBW make the whole configuration suitable to communicate simultaneously with several earth stations located in different places.

Table 3 - design characteristics and achieved results at X-band.

Characteristics	Slot antenna design	Full system
Dielectric constant (Teflon)	2.1	2.1
Dielectric thickness (Teflon)	1.2 mm	1.2 mm
Physical size	37 mm × 37 mm	37 mm × 37 mm
Operating frequency	8.40 GHz	8.40 GHz
Return Loss (8.4 GHz)	~ 20.0	~20.0
VSWR (8.4 GHz)	Close to one	Close to one
Beamwidth angle (8.4 GHz)	×	Very wide
Radiation Pattern (8.4 GHz)	Bidirectional	Unidirectional
Back lobes (8.4 GHz)	Important	minimum
Gain (8.4 GHz)	5.91 dBi	~11.0 dBi

Table 4 - Suitability for CubeSats at X-band (8.40 GHz).

Characteristics	Full System
Surface / 0.5U CubeSat's top face (10×5 cm ²)	27.38%
Volume / 0.5U CubeSat's volume	3.28%
Surface / 1U CubeSat's top face (10×10 cm ²)	13.69%
Volume / 1U CubeSat's volume	1.642%
Surface / 2U CubeSat's top face (10×20 cm ²)	6.84%
Volume / 2U CubeSat's volume	0.821%
Surface / 3U CubeSat's top face (10×30 cm ²)	4.56%
Volume / 3U CubeSat's volume	0.547%
Surface / 6U CubeSat's top face (20×30 cm ²)	2.28%
Volume / 6U CubeSat's volume	0.2.73%
Power consumption	Very low
Radiation	Directional antenna
Beamwidth Angle	Very wide
Interferences with CubeSat subsystems	Minimum
Power dissipation	Negligible
Gain	~11.0 dBi
Cost	Very low (<10 \$)
Mass	Lightweight
Suitability for All CubeSat Configurations	Very suitable

From another hand, tables 5, 6 and 7 compare the constructed antenna system with similar antenna designs that can be used for CubeSats in terms of their geometrical parameters or electrical properties. Not that the suitability for a CubeSat mission is studied in terms of geometrical, mechanical and electrical characteristics of proposed antennas. Therefore, an antenna system can be used for a CubeSat configuration if it satisfies all geometrical, mechanical and electrical requirements of the CubeSat mission. Compared to all antenna systems developed in (Paiva et al., 2019; Naqvi & Lim, 2018; Chaimool et al., 2019; Gupta et al, 2018), our suggested BTSA design provides the maximum gain with extremely high stiffness, smallest area, and lowest volume. Furthermore, its cheap cost makes our BTSA system the best choice for infinite lifespan CubeSat missions employing all CubeSat designs, like the UM5-Ribat and UM5-EOSAT CubeSats of University Mohammed V in Rabat. On the other hand, the works presented in (Paiva et al., 2019; Naqvi & Lim, 2018; Chaimool et al., 2019; Gupta et al, 2018) used metasurfaces to improve radiating properties, and therefore the chance of mission collapse is too high due to their weight and poor stiffness. Furthermore, the

small size of our BTSA design allows the CubeSat constructor to install more solar arrays on the aluminum chassis of the proposed 2U CubeSat to generate as much electric power as possible, thereby increasing the productivity of functions scheduled for small and medium-sized CubeSat missions. Furthermore, our suggested BTSA system is powered by a simple 50Ω strip line, requiring less power, which is restricted on CubeSats and tiny spacecraft. This is critical for CubeSats since it provides electrical energy to the other CubeSat circuits, increasing both the satellite's lifetime and mission output.

Table 5 - Comparison of propose BTSA and some works that used Metasurfaced antenna designs.

Reference	(Paiva et al., 2019)	(Naqvi & Lim, 2018)	(Chaimool et al., 2019)	(Gupta et al, 2018)	Our works
Frequency	2.45 GHz	2.45 GHz	2.45 GHz	11.40 GHz	8.40 GHz
Size in mm ²	96.5×96.5	120×120	80×80	100×100	37 ×37
Dielectric Material	RO4350	FR4 / RO3003	FR-4	FR-4	Teflon
Feeding System	50Ω strip line	50Ω aperture coupled feed	50Ω strip line	50Ω coaxial probe	50Ω strip line
Antenna Approach / Technology	Metasurface + Use of a 45° chamfered square ring shape in the upper left and lower right corners of unit cells	2 microfluidic metasurfaces + Injection of liquid metal (EGaIn) + Use of polydimethylsiloxane (PDMS)	Reconfigurable Metasurface + PIN diode bias	Minkowski fractal-shaped metamaterial (MTM) + defected ground plane	Quasi Newtonian Method (QNM) + Use of 2U CubeSat top face as reflector
RL (dB)	33.0	~ 14.0	~ 27.0	28.1	~ 20.0
Radiation Pattern	Unidirectional (Main lobe +low back lobe)	Bidirectional (Main lobe ~ back lobe)	Bidirectional (Main lobe + back lobe)	Multi-lobes: Main lobe + 2 side lobes + 3 back lobes	Unidirectional (Main lobe +very low back lobe)
Peak Gain	5.69 dBi	~6.0 dBi	~ 6.0 dBi	8.9 dBi	~11.0 dBi
Stiffness	Low	Low	Low	Low	Very High
CubeSat Standard	3U	6U	3U	3U	2U
Interferences	low	√	√	√	minimum
Power Losses	Low	Important	Important	important	minimum
Orbits (mile)	Low orbits	×	×	×	Medium & deep orbits

The antenna design that the authors of (Panda et al., 2020) have presented is geometrically unsuited for any CubeSat configuration because of its greater dimensions in relation to 1U, 2U, and 3U standards, as well as its relatively poor gain for 6U CubeSats, which are mostly utilized for interplanetary purposes. Furthermore, if the 6U arrangement is recommended and the link can be guaranteed by utilizing extremely high gain earth segments, it provides a multi-lobe radiation pattern that permits large interferences with other components. The antenna configurations presented in (Samantaray & Bhattacharyya, 2020) (Kaur & Kaur, 2019) (Mahendran et al., 2021) meet all of the geometrical and mechanical requirements for any CubeSat configuration. However, because of their multilobe radiation pattern, their main drawback—which prevents them from being used in space—is the extremely high interference they cause with other circuits inside the satellite box. Conversely, their gains fall short of 10 dBi, which is why our BTSA design achieves the highest gain at X-band while maintaining the lowest cost and volume. Although the antenna systems described in contributions (Ali et al., 2018) (Anand & Chawla, 2020) (Bag et al., 2020) (Bhattacharya et al., 2021) (Han et al., 2020) (Eslami et al., 2021) (Mishra, 2019) (Srivastava et al., 2020) (Salamin et al., 2019) (Tewary et al., 2021) (Sahoo et al., 2018) satisfy all geometrical and mechanical requirements for all CubeSat standards, their extreme back lobe radiation limits their applicability for use on CubeSats. They have extremely high failure rates because to their high losses and strong interference tolerance. The extremely low return loss and poor gain at X-band of the antenna design created by the authors of (Mishra & Mangaraj, 2019) make it unsuitable for integration

with CubeSats, despite its unidirectional radiation pattern, compact size, and strong rigidity. Similarly, it results in significant electrical energy losses that are severely limited on CubeSats.

Table 6 - Geometrical comparison of the proposed BTSA with some Patch antenna designs at X-band

Reference	F ₀ in GHz	Volume [mm ³]	Dielectric Material	Feeding System
(Panda et al., 2019)	10	380 × 148 × 1.6	FR4	50Ω strip line
(Samantaray & Bhattacharyya, 2020)	10.94	28×28×8.4	FR4	50Ω strip line
(Kaur & Kaur, 2019)	9.6	27.5×42.5×1.57	FR4	50Ω strip line
(Mahendran et al., 2021)	9.7	50×30×1.6	FR4	50Ω strip line
(Ali et al., 2018)	10.44	35 × 30 × 1.6	FR4	50Ω strip line
(Anand & Chawla, 2020)	8.2	40×40×3.2	FR4	50Ω strip line
(Bag et al., 2020)	8.94	50×30×1.6	FR4	50Ω strip line
(Bhattacharya et al., 2021)	10	46.7×46.7×3.2	FR4	4 Apertures
(Han et al., 2020)	10	13.39×9.16×4.4	Rogers RO3003	50Ω CPW line
(Eslami et al., 2021)	8.95	34×36×1.6	FR4	50Ω strip line
(Mishra, 2019)	11	32×32×1.6	FR4	50Ω strip line
(Srivastava et al., 2020)	9	25×26×1.6	FR4	50Ω strip line
(Salamin et al., 2019)	10.8	52.8 ×52.8× 21.2	FR4	50Ω strip line
(Tewary et al., 2021)	8.15	37×35×3.4	Laminate	Aperture
(Sahoo et al., 2018)	9	13×14×1.5	FR4	50Ω strip line
(Yadav et al., 2020)	8.19	80×36×1.575	RT-Duroid 5880	50Ω SIW line
(Chen & Shie, 2019)	9.2	40× 30× 5.1	RT-Duroid 5880	50Ω strip line
(Mishra & Mangaraj, 2019)	9	20×20×2.5	FR4	50Ω coaxial probe
(Prabhu et al., 2020)	9.3	8×16×4.8	FR4	50Ω coaxial probe
(Bhongale, 2019)	10.5	22.5×22.5×2	Mg-Nd-Cd ferrite	50Ω coaxial probe
Our work	8.4	37×37×1.2	Teflon	50Ω strip line

Table 7 - Electrical comparison of the proposed BTSA with some Patch antenna designs at X-band

Reference	F ₀ in GHz	RL [dB]	Radiation Pattern	Peak Gain	Power Losses
(Panda et al., 2019)	10	46.25	Multi-Lobes	4.52 dBi	High
(Samantaray & Bhattacharyya, 2020)	10.94	~ 25	Multi-Lobes	8.17 dBi	High
(Kaur & Kaur, 2019)	9.6	~ 40	Multi-Lobes	~4 dBi	High
(Mahendran et al., 2021)	9.7	~ 25	Multi-Lobes	2.09 dBi	High
(Ali et al., 2018)	10.44	~ 23	Bidirectional	~7.5 dBi	High
(Anand & Chawla, 2020)	8.2	~ 28	Bidirectional	7.023 dBi	High
(Bag et al., 2020)	8.94	~ 30	Bidirectional	~5.5 dBi	High
(Bhattacharya et al., 2021)	10	~ 30	Bidirectional	2.5 dBic	Very High
(Han et al., 2020)	10	26	Bidirectional	6.72 dBi	High
(Eslami et al., 2021)	8.95	15	Bidirectional	2.63 dBi	Very High
(Mishra, 2019)	11	~ 15	Bidirectional	2.2 dBi	High
(Srivastava et al., 2020)	9	~ 25	Bidirectional	6.2 dBi	High
(Salamin et al., 2019)	10.8	~ 27	Bidirectional	~3 dBi	High
(Tewary et al., 2021)	8.15	~ 22	Bidirectional	5.33 dBi	High
(Sahoo et al., 2018)	9	~ 25	Bidirectional	~2.2 dBi	Very High
(Yadav et al., 2020)	8.19	~ 25	unidirectional	9.6 dBi	Medium
(Chen & Shie, 2019)	9.2	~ 38	unidirectional	7.8 dBi	medium
(Mishra & Mangaraj, 2019)	9	low	unidirectional	Not assigned	high
(Prabhu et al., 2020)	9.3	~ 28	unidirectional	~8 dBi	low
(Bhongale, 2019)	10.5	~ 30	unidirectional	0.46 dBi	Low
Our work	8.4	~ 20	unidirectional	~11 dBi	Negligible

The antenna approach described in (Bhongale, 2019) results in a relatively low gain at X-band (0.46 dBi), which can only be utilized for specific nearfield applications under specified conditions. As a result, it does not meet the suitability criterion for CubeSat missions. Compared to antenna systems created in (Yadav et al., 2020) (Chen & Shie, 2019), our configured Bow Tie

slot antenna design allows for greater gain, occupies the smallest volume, consumes very little electric energy, and is a low-cost CubeSat antenna system. Furthermore, our created BTSA system has a substantial advantage over the antenna system developed using the technique of (Prabho et al., 2020) because to its minimal power losses, greater gain, lightweight, and low-cost design. As a consequence, our Bow Tie Slot antenna solution outperforms all other listed antenna techniques, meeting all CubeSat requirements.

5. Conclusions and Future Works

In this study, a Bow Tie Slot antenna design integrated with a 2U CubeSat integration is suggested for the first time. It is small size, lightweight, low power consumption, and highly compatible with all CubeSat configurations, including 0.5U, 1U, 1.5U, 2U, and 3U. Additionally, in order to improve its stiffness and radiation properties, such as the antenna boresight gain and HPBW at 8.4 GHz (X-band), the air-gap distance is lowered to only 1 mm. It is discovered that the devised method offers a very broad HPBW of almost 160° at 8.4 GHz, a unidirectional radiation pattern, and a peak gain of about 11.0 dBi. Besides that, employing small-sized CubeSat designs as UM5-Ribat and UM5-EOSAT of University Mohammed V in Rabat, broad bandwidths of 430 MHz and substantial return losses are generated at the same X-band operating frequency, increasing its usefulness for CubeSat communications.

References

- Abels, J. (2024). Private infrastructure in geopolitical conflicts: the case of Starlink and the war in Ukraine. *European Journal of International Relations*. <https://doi.org/10.1177/13540661241260653>.
- Ali, T., Fatima, N., & Biradar, R. C. (2018). A miniaturized multiband reconfigurable fractal slot antenna for GPS/GNSS/Bluetooth/WiMAX/X-band applications. *AEU - International Journal of Electronics and Communications*, *94*, 234-243. <https://doi.org/10.1016/j.aeue.2018.07.017>.
- Anand, R., & Chawla, P., (2020). A novel dual-wideband inscribed hexagonal fractal slotted microstrip antenna for C- and X-band applications. *Inter. Journal RF Microwave Computer Aided Eng.*, *30*(9), e22277. <https://doi.org/10.1002/mmce.22277>.
- Bag, B., Biswas, P., De, S., Biswas, S., & Sarkar, P.P., (2020). A Wide Multi-band Monopole Antenna for GSM/WiMAX/WLAN/X-Band/Ku-Band Applications. *Wireless Pers. Commun.*, *111*, 411–427. <https://doi.org/10.1007/s11277-019-06866-1>.
- Bhattacharya, A., Dasgupta, B., & Jyoti, R. (2021). Design and analysis of ultrathin X-band frequency selective surface structure for gain enhancement of hybrid antenna. *Inter. Journal RF Microw Comput Aided Eng.*, *31*(2), e22505. <https://doi.org/10.1002/mmce.22505>.
- Bhongale, S.R. (2019). Mg-Nd-Cd Ferrite as Substrate for X-Band Microstrip Patch Antenna. *Journal of Magnetism and Magnetic Materials*, *499*, 165918. <https://doi.org/10.1016/j.jmmm.2019.165918>.
- Campioli, S., Stesina, F., La Bella, E., Corpino, S., Niero, L. & My, C. (2024). Concurrent Engineering to Enhance Autonomy for Deep-Space CubeSat Mission Design. *IFAC-PapersOnLine*, *58*(16), 163-168. <https://doi.org/10.1016/j.ifacol.2024.08.480>.
- Chaimool, S., Hongnara, T., Rakluea, C., Akkaraekthalin, P., & Zhao, Y. (2019). Design of a PIN Diode-Based Reconfigurable Metasurface Antenna for Beam Switching Applications. *International Journal of Antennas and Propagation*, *2019*, 72163224, 1-7. <https://doi.org/10.1155/2019/7216324>.
- Chen, S. L., & Shie, M. H. (2019). A Compact High Gain X-Band Patch Antenna for Cube and Small Satellite Applications. *Proceeding of the IEEE International Symposium on Antennas and Propagation and USNC-URSI Radio Science Meeting*, 1561-1562. <https://doi.org/10.1109/apusncursinrsm.2019.8888759>.
- Chu, C., Wang, M., Wang, J., Guo, Y., & Wu, W. (2023). A New Design of Filtering Patch Antennas With Enhanced Bandwidth and Harmonic Suppression. In *IEEE Transactions on Antennas and Propagation*, *71*(7), 6120-6125. [10.1109/TAP.2023.3266059](https://doi.org/10.1109/TAP.2023.3266059).

- Cratere, A., Gagliardi, L., Sanca, G.A., Golmar, F., & Dell'Olio, F. (2024). On-Board Computer for CubeSats: State-of-the-Art and Future Trends. *IEEE Access*. <https://doi.org/10.1109/ACCESS.2024.3428388>.
- El Bakkali, M. (2020). Planar Antennas with Parasitic Elements and Metasurface Superstrate Structure for 3U CubeSats, PhD. *Thesis*, Sidi Mohamed Ben Abdellah University, city of Fez, Morocco.
- El Bakkali, M., Bekkali, M. E., Gaba, G. S., Guerrero, J. M., Kansal, L., & Masud, M. (2021). Fully Integrated High Gain S-Band Triangular Slot Antenna for CubeSat Communications. *electronics*, *10*(2), 156. <https://doi.org/10.3390/electronics10020156>.
- Eslami, A., Nourinia, J., Ghobadi, C., & Shokri, M. (2021). Four-element MIMO antenna for X-band applications. *International Journal of Microwave and Wireless Technologies*, *13*(8), 859–866. <https://doi.org/10.1017/s1759078720001440>.
- Francisco, C., Henriques, R., & Barbosa, S. (2023). A Review on CubeSat Missions for Ionospheric Science. *Aerospace*, *10*(7), 622. <https://doi.org/10.3390/aerospace10070622>.
- Giannetti, G. (2023). Improved and easy-to-implement HFSS-MATLAB interface without VBA scripts: an insightful application to the numerical design of patch antennas. *Applied Computational Electromagnetics Society Journal*, *38*, 377-381. <https://hdl.handle.net/2158/1354802>.
- Gupta, N., Saxena, J., Bhatia, K. S., & Dadwal, N. (2018). Design of Metamaterial-Loaded Rectangular Patch Antenna for Satellite Communication Applications. *Iranian Journal of Science and Technology, Trans. of Electr. Eng.*, *43*, 39-49. <https://doi.org/10.1007/s40998-018-0118-9>.
- Han, Y., Gong, S., Wang, J., Li, Y., Qu, S., & Zhang, J. (2020). Reducing RCS of Patch Antennas via Dispersion Engineering of Metamaterial Absorbers. *IEEE Transactions on Antennas and Propagation*, *68*(3), 1419-1425. <https://doi.org/10.1109/tap.2019.2925275>.
- Huang, X., Chen, P., & Xia, X. (2024). Heterogeneous optical network and power allocation scheme for inter-CubeSat communication. *Optics Letters*, *49*(5), 1213-1216. <https://doi.org/10.1364/OL.514198>.
- Jardak, N., & Adam, R. (2023). Practical Use of Starlink Downlink Tones for Positioning. *Sensors*, *23*(6), 3234. <https://doi.org/10.3390/s23063234>.
- Kaur, N., & Kaur, A. (2019). A Compact Plus Shaped Carpet Fractal Antenna with an I-Shaped DGS for C-band/X-band/UWB/WIBAN applications. *Wireless Pers. Commun.*, *109*, 1673–1687. <https://doi.org/10.1007/s11277-019-06645-y>.
- Kogut, A., Annino, G., Bakkali, M. E., Laamara, R. A., Arora, S. K., Naik, D. S. B., & Maniraguha, F. (2022). Millimeter Wave All-Around Antenna Based on Whispering Gallery Mode Dielectric Resonator for IoT-Based Applications. *Wireless Communications and Mobile Computing*, *2022*(1), 5877263, 1-10. <https://doi.org/10.1155/2022/5877263>.
- Li, X., Ma, R., Cai, H., Pan, Y. -M., & Zhang, X. Y. (2023). High-Gain Dual-Band Aperture-Shared CP Patch Antenna With Wide AR Beamwidth for Satellite Navigation System. In *IEEE Antennas and Wireless Propagation Letters*, *22*(8), 1888-1891. <https://doi.org/10.1109/LAWP.2023.3268653>.
- Liu, T., & Feng, Q. (2023). Broadband and High-Gain Low-Profile Array Antenna Loaded With Parasitic Patches. In *IEEE Antennas and Wireless Propagation Letters*, *22*(10), 2595-2599. <https://doi.org/10.1109/LAWP.2023.3298364>.
- Liu, G., Hu, P. F., Su, G. D., & Pan, Y. M. (2024). Bandwidth and Gain Enhancement of a Single-Layer Filtering Patch Antenna Using Reshaped TM Mode. In *IEEE Antennas and Wireless Propagation Letters*, *23*(1), 314-318. <https://doi.org/10.1109/LAWP.2023.3323653>.
- Mahendran, K., Gayathiri, R., & Sudarsan, H. (2021). Design of Multi Band Triangular Microstrip Patch Antenna with Triangular Split Ring Resonator for S Band, C Band and X Band Applications. *Microprocessors and Microsystems*, *80*, 103400. <https://doi.org/10.1016/j.micpro.2020.103400>.
- Mishra, B. (2019). An ultra compact triple band antenna for X/Ku/K band applications. *Microw Opt Technol Lett.*, *61*(7), 1857–1862. <https://doi.org/10.1002/mop.31812>.

- Mishra, G.P., & Mangaraj, B.B. (2019). Miniaturised microstrip patch design based on highly capacitive defected ground structure with fractal boundary for X-band microwave communications. *IET Microw. Antennas Propag.*, 13(10), 1593-1601. <https://doi.org/10.1049/iet-map.2018.5778>.
- Naqvi, H., & Lim, S. (2018). Microfluidically Polarization-Switchable Metasurfaced Antenna. *IEEE Antennas and Wireless Propagation Letters*, 17(12), 2255-2259. <https://doi.org/10.1109/lawp.2018.2872108>.
- Paiva, J. L. d. S., Silva, J. P. D., Campos, A. L. P. d. S., & Andrade, H. D. D. (2019). Using metasurface structures as signal polarisers in microstrip antennas. *IET Microwaves, Antennas Propagation*, 13(1), 23-27. <https://doi.org/10.1049/iet-map.2018.5112>.
- Patidar, H., Das A., & Kar, R. (2024). Small planar antenna array design using length and spacing through Matlab-HFSS interfacing. *International Journal of Communication Systems*, 37(9), e5770.
- Panda, R. A., Panda, M., Nayak, P. K., & Mishra, D. (2020). Log periodic implementation of butterfly shaped patch antenna with gain enhancement technique for X-band applications. In *ICICCT 2019–System Reliability, Quality Control, Safety, Maintenance and Management: Applications to Electrical, Electronics and Computer Science and Engineering* (pp. 20-28). Springer Singapore.
- Prabhu, T., Suganya, E., & Pandian, S. C. (2020, March). Design of an UWB antenna for Microwave C and X Band Applications. In *2020 6th International Conference on Advanced Computing and Communication Systems (ICACCS)* (pp. 311-316). IEEE.
- Sahoo, A.K., Gupta, R.D., & Parihar, M.S. (2018). Circularly polarised filtering dielectric resonator antenna for X-band applications. *IET Microwaves, Antennas & Propagation*, 12(9), 1514-1518. <https://doi.org/10.1049/iet-map.2017.1159>.
- Samantaray, D., & Bhattacharyya, S. (2020). A Gain-Enhanced Slotted Patch Antenna Using Metasurface as Superstrate Configuration. *IEEE Transactions on Antennas and Propagation*, 68(9), 6548-6556. <https://doi.org/10.1109/tap.2020.2990280>.
- Srivastava, K., Mishra, B., Patel, A.K., & Singh, R. (2020). Circularly polarized defected ground stub-matched triple-band microstrip antenna for C- and X-band applications. *Microwave and Optical Technology Letters*, 62(10), 3301-3309. <https://doi.org/10.1002/mop.32450>.
- Salamin, M. A., Ali, W. A.E., Das, S., & Zugari, A. (2019). Design and investigation of a multi-functional antenna with variable wideband/notched UWB behavior for WLAN/X-band/UWB and Ku-band applications. *AEU-International Journal of Electronics and Communications*, 111, 152895. <https://doi.org/10.1016/j.aeue.2019.152895>.
- Tewary, T., Maity, S., Mukherjee, S., Roy, A., Sarkar, P. P., & Bhunia, S. (2021). Design of high gain broadband microstrip patch antenna for UWB/X/Ku band applications. *AEU-International Journal of Electronics and Communications*, 139, 153905. <https://doi.org/10.1016/j.aeue.2021.153905>.
- UM5-Ribat & UM5-EOSat CubeSats. (2024). *Website of Space Watch Africa*, Retrieved from: <https://spacewatchafrica.com/mohammed-v-university-and-spacex-launch-two-nanosatellites/> [Retrieved on: 23th September 2024].
- Voštinár, P., & Ferienc, P. (2023). Merge Cube as a New Teaching Tool for Augmented Reality, *IEEE Access*, 11, 81092-81100. <https://doi.org/10.1109/ACCESS.2023.3301399>.
- Yadav, M. V., Baudha, S., and Singam, S. C. (2020). Multiple Slot Planar Antenna for X-Band Satellite Mobile Communication. *Proceeding of the IEEE 7th Uttar Pradesh Section International Conference on Electrical, Electronics and Computer Engineering (UPCON)*, 1-4. <https://doi.org/10.1109/upcon50219.2020.9376539>.
- Zea, L., Aguilar-Nadalini, A., Martínez, M., Birnie, J., Miranda, E., España, F., Chung, K., Álvarez, D., Bagur, J. A., Estrada, C., Herrarte, R., & Ayerdi, V. H. (2023). Academic development and space operations of a multispectral imaging payload for 1U CubeSats. *Journal of Applied Remote Sensing*, 17(4), 047501-047501. <https://doi.org/10.1117/1.JRS.17.047501>.
- Zhang, S., Liu, N. -W., Li, Y., & Sun, S. (2023). A Gain-Enhanced Differential-Fed Stacked Circular Patch Antenna With Simultaneously Controllable E-Plane and H-Plane

Radiation Nulls. *IEEE Transactions on Antennas and Propagation*, 71(8), 6399-6412.
<https://doi.org/10.1109/TAP.2023.3284047>.